Journal of Materials Chemistry B

Accepted Manuscript

ROYAL SOCIETY OF CHEMISTRY

www.rsc.org/materialsB

Journal of Materials Chemistry B

PAPER

Optimized effective charge density and size of polyglycerol amines leads to strong knockdown efficacy *in vivo*

Received 00th January 20xx,
Accepted 00th January 20xx

DOI: 10.1039/x0xx00000x

www.rsc.org/

Anna Maria Staedtler, [†,a] Markus Hellmund, [†,b] Fatemeh Sheikhi Mehrabadi, [b] Bala N. S. Thota, [b] Thomas M. Zollner, [a] Markus Koch, [a] Rainer Haag [b,*] and Nicole Schmidt [a,*]

RNA interference (RNAi)-based therapy extends the range of "druggable" targets beyond existing pharmacological drugs and enables the development of new treatment strategies for various diseases. A prerequisite are non-viral polyvalent gene delivery vectors capable for safe and effective siRNA delivery to cells *in vivo* allowing a broad clinical application. We synthesized hyperbranched polyglycerol amines (hPG amines) which varied in their charge density, multiplicity (absolute frequency of amine groups) and core size to successfully develop potent and safe siRNA transfer vectors. The characterization of hyperbranched polyglycerol amines with an invariable core size (8kDa) but different amine loading revealed a correlation between the effective charge density and the transfection efficacy without impacting the cell viability *in vitro*. However, this correlation was not seen in tumor bearing mice *in vivo* treated with 8kDa hPG amine-siRNA complexes. Improving the effective charge density and the multiplicity of amine functionalities by increasing the molecular weight (43kDa) revealed comparable transfection efficacy *in vitro* but less toxic side effects after systemic administration *in vivo* compared to the respective hPG amine (8kDa). In addition, *in vivo* delivery of 43kDa hPG amine-siRNA-polyplexes in tumors resulted in a highly specific and significant knockdown effect. These findings demonstrate that hyperbranched polyglycerol amines with a balanced effective charge density, multiplicity and core size are promising gene delivery vectors for siRNA therapy which enable to address so far "undruggable" targets due to high tolerability and effective siRNA delivery.

Introduction

RNA interference (RNAi) is a process of sequence-specific post-transcriptional gene silencing triggered by small interfering RNAs (siRNAs).[1] Therapeutic applications of siRNA offer an endogenous and highly efficient strategy to address so far "undruggable" targets.[2,3] A key advantage of siRNA drug development is the possibility to synthetically generate siRNA which can target and silence virtually any class of genes (including both protein-encoding genes and non-coding RNAs), providing a broader therapeutic application than common protein-based drugs.[4,5] However, the success of gene silencing applications based on synthetic siRNA critically depends on efficient intracellular transfer. Hence, there is an urgent need for potent siRNA delivery systems.[6]

In the last decades viral and non-viral gene delivery vectors have been critically studied concerning their properties of siRNA delivery.[4,7–9] To date, the up-concentration of nanoparticles in the liver used for gene delivery and thus the cause of undesired problems, leads to investigations on neutral or negatively charged lipid formulations, like the 2nd generation of lipid nanocarriers or even glycolproteins like trivalent (triantennary) N-acetylgalactosamine (GalNAc). These candidates are promising carrier systems in clinical trials. Although, viral vectors are highly efficient at delivering genetic material, they often exhibit immunogenicity and mutagenicity or suffer from expensive and laborious production in large scale quantities. In contrast, non-viral gene delivery vectors, based on lipids or cationic polymers, can provide a number of promising advantages including stability, low immunogenicity and toxicity, which make them highly suitable for *in vivo* applications.[8,10–12] Since cationic lipids based on glycerol-backbone and the lipid-DOTMA were successfully used as delivery vectors for plasmid-DNA, the field of cationic lipids has been widely explored.[12–14] Furthermore, the development of different headgroups and their influence on transfection efficacy was studied.[15] Nowadays, cationic lipids are commercially available as transfection reagents for laboratory use, especially as technical controls, e.g. lipofectamin. Beside cationic lipids, cationic polymers, like PAMAM (poly(amindoamine)) and PEI (poly(ethylenimine)), show excellent transfection rates due to efficient endocytosis and the "proton sponge effect",[16] but with increased size and charge density their toxic side effects enhance as well.[17] As a

[a] Bayer Healthcare, GDD, Global Therapeutic Research, TRG Oncology/ Gynecological Therapies, Muellerstr. 178, 13353 Berlin, Germany, Tel: +49 30 468 194360, Email: nicole.schmidt1@bayer.com
[b] Institut für Chemie und Biochemie, Freie Universität Berlin, Takustr. 3, 14195 Berlin, Germany, Tel.: +49 30 838 52633, Email: haag@chemie.fu-berlin.de
† Both authors are contributing equally
Electronic Supplementary Information (ESI) available:See DOI: 10.1039/x0xx00000x

result, low molecular weight PEI was used trying to avoid toxicity.[18,19] However, the high charge density on these smaller PEI can induce necrosis and/or apoptosis due to destabilization of the membrane, or inhibit normal cellular processes.[20,21] So far, the influence of structural modifications on the positive charge of different PAMAM- and PEI-derivates was indicated by published *in vitro* and *in vivo* studies.[22–25] In addition, less toxic cationic polyglycerol derivatives were analyzed regarding their ability to deliver siRNA *in vitro* and *in vivo*.[26,27] It was reported that the presentation of multiple amine groups on the surface caused effective and strong binding to nucleic acids, however, neither the toxic profile nor the fast clearance could be improved. In this work, we hypothesize that the optimization of the effective charge density in combination with multiplicity will increase the therapeutic window between toxic side effects and transfection efficacy. Taking advantage of the characteristic that hyperbranched polyglycerol-based gene delivery vectors can be adjusted in size, charge and multiplicity, different hPG amines with varying amine densities and molecular weights were investigated and analyzed concerning their effective charge density as well as their tolerability and knockdown efficacy *in vitro* and *in vivo*.

Results and Discussion

Evaluation of the effective charge density using hPG amines

The stability of complexes consisting of siRNA molecules and cationic polymers (defined as polyplex) is mainly dependent on the charge density, the size of the polymeric scaffold, the multiplicity and the way of charge presentation on the outer sphere.[26–28] Thereby, hyperbranched polyglycerol (hPG) benefits from the location of the majority of its functional groups (60%) on the surface.[29] To evaluate the role of the effective charge density and the multiplicity of hPG amines on their potency to deliver genetic material, we designed different hPG amines with varied effective charge densities on the same core or increased core size, respectively. Based on a molecular weight of the polyglycerol core of Mn 8kDa, three different hPG amines with different amine loading were synthesized, 8kDa PG90 (90% amine loading), 8kDa PG70 (70% amine loading) and 8kDa PG50 (50% amine loading), according to the published three step protocol.[30] Since the effective charge density is limited due to the small core size, another hPG core with a five times higher molecular weight (Mn 43kDa) was synthesized fulfilling the aim to further increase the effective charge density and multiplicity (Scheme 1). The multiplicity of amine groups is thereby defined as the total amine group amount per surface area per particle.

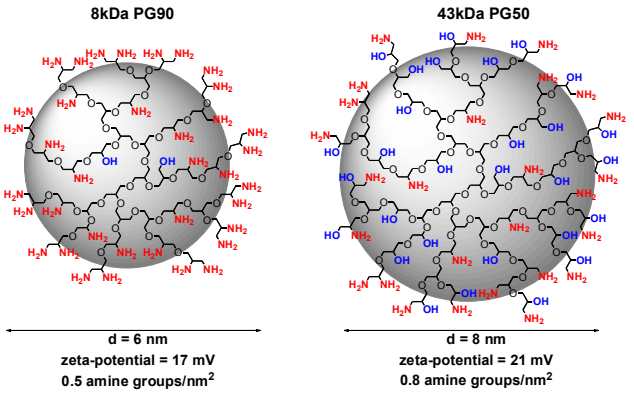

Scheme 1. Schematic structural difference of PG90 8kDa and PG50 43kDa. Both hPG amines are varying in size, charge and amount of the total amine groups (labeled in red).

Hence, the hydrodynamic size of the core was increased from 6 nm (8kDa PG) to 8 nm (43kDa PG) still enabling renal clearance to avoid severe toxic risks.[13,31] Subsequently, two different 43kDa hPG amines with varying amine loadings were synthesized: 43kDa PG30 (30% amine loading) and 43kDa PG50 (50% amine loading).To confirm that the effective charge density is not only affected by the total amount of amine groups but also by the core size, the zeta-potential of the polymeric scaffolds was determined, 8kDa PG50 (15.5±0.9 mV), 8kDa PG70 (16.7±0.9 mV), 8kDa PG90 (17.2±1.3 mV), 43kDa PG30 (19.3±1.9 mV) and 43kDa PG50 (21.3±0.6 mV). Here, the total amount of amino groups clearly correlated with the effective charge density and the core size of the evaluated nanoparticles (Figure 1).

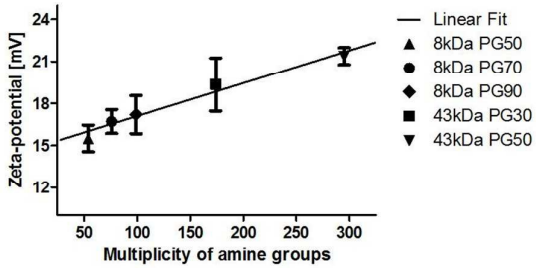

Figure 1. Correlation between the multiplicity of amine groups and the zeta-potential of different uncomplexed hPG amines. Zeta-potential is shown as mean±SD of at least triplicates measured in PBS buffer. The r^2 distribution was used for testing the goodness of fit: r^2=0.9692.

Evaluation of transfection efficacy *in vitro* and *in vivo* of 8kDa hPG amines

In order to investigate the influence of the amine multiplicity of the 8kDa hPG amines on transfection efficacy, their complexation capacity of siRNA at different N/P ratios was determined using gel electrophoresis, measurement of the zeta-potential and hydrodynamic size (DLS) (Supporting Information, Figure S 1 and Figure S 2). The gel electrophoresis studies revealed an efficient complexation for all 8 kDa hPG

amines with siRNA molecules starting at N/P 3 indicated by no migration toward the positive pole vs. pure siRNA. The DLS and zeta potential measurements performed for the 8kDa hPG amines showed a decreased by 5-11 mV starting at N/P 1 compared to the pure 8kDa hPG amines in consequence of the neutralization induced by the polyplex formation (Supporting Information, Figure S 2). This observation was confirmed by the determination of the hydrodynamic size of the 8kDa polyplexes revealing a constant diameter starting at N/P 3. Based on these physicochemical characterizations and considering the impact of the amine multiplicity on transfection efficacy, N/P ratio of 10 for 8kDa PG50, 8 for 8kDa PG70 and 3 for 8kDa PG90 were selected to characterize the 8kDa hPG amines regarding their safety and transfection efficacy. For this purpose the human renal carcinoma cell line 786-O-Luc consistently expressing luciferase as a reporter gene was used. The siRNA-mediated knockdown of the luciferase gene followed by reduced luciferin-triggered light emission defined the transfection efficacy of the tested nanoparticles. All 8kDa hPG amines complexes were non-toxic with no significant effect on cell viability assessed by the ONE-Glo™ assay *in vitro* (Supporting Information, Figure S 4A). To determine the transfection efficacy of the 8kDa hPG amine complexes, 786-O-Luc cells were transfected with non-targeting siRNA and luciferase specific siRNA and changes of the luciferase activity were measured. Incubation of 8kDa hPG amine complexed with non-targeting siRNA revealed no inhibitory effect on luciferase activity compared to control (Supporting Information, Figure S 4B). In contrast, 8kDa hPG amines complexed with anti-Luc siRNA induced notable knockdown effects in dependence on their amine loading. 8kDa PG50 inhibited the luciferase activity by 20%, while 8kDa PG70 caused a decrease of 41% luciferase activity compared to control. Notably, 8kDa PG90 complexed with anti-Luc siRNA revealed the most target-specific and strongest knockdown effect of 45% vs. control. Our results show that 8kDa hPG amine polyplexes do not affect cell viability but show transfection efficacy correlated to the increased effective charge density.

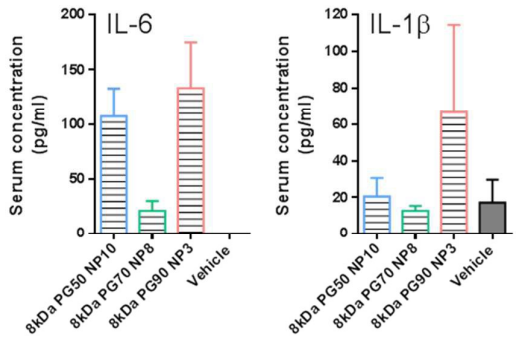

Figure 2. Determination of pro-inflammatory cytokine levels after systemic administration of 8kDa hPG amines: three BALB/c mice per group were treated intravenously with 8 mg/kg 8kDa PG50, 8kDa PG70 or 8kDa PG90, complexed with non-targeting siRNA (ON-TARGETplus Non-targeting siRNA, Dharmacon) at N/P ratios of 10, 8, and 3, respectively. HyClone™ HyPure water was used as negative control (vehicle). Retrobulbar blood was taken 1h after injection and serum was analysed via Meso Scale Discovery Multi-Spot Assay System, Mouse ProInflammatory 7-Plex Assay Ultra-Sensitive Kit. Results are shown as mean±SD of triplicates.

Furthermore, we investigated the impact of the effective charge density on the tolerability and transfection efficacy *in vivo*. The administration of nanotransporters is unfortunately often restricted *in vivo* due to the activation of the innate immune response leading to the secretion of pro-inflammatory cytokines.[32] Hence, 8kDa PG50, 8kDa PG70 and 8kDa PG90 polyplexes have been evaluated regarding their acute effect on pro-inflammatory cytokine levels after intravenous administration (Figure 2 and Supporting Information, Figure S 5). Therefore, blood was taken 1h after administration and pro-inflammatory cytokines, i.e. IL-6 and IL-1β (Figure 2), were determined in the serum using Meso Scale Discovery Multi-Spot Assay System. All 8kDa hPG polyplexes enhanced the levels of IL-6 vs. control. Especially 8kDa PG50 and 8kDa PG90 revealed the strongest increase of IL-6 in the serum in comparison to vehicle. The secretion of IL-1β was not influenced by 8kDa PG50 and 8kDa PG70 but increased by 8kDa PG90 vs. vehicle. In conclusion, the administration of hPG amines especially 8kDa PG90 caused an induction of the pro-inflammatory cytokines IL-6 and IL-1β compared to the control HyClone™ HyPure water. However, these increased levels are not comparable to published changes associated with severe immune toxicity,[33,34] but indicating dose limitations for *in vivo* administration. Therefore, *in vivo* transfection efficacy studies have been performed with 8 mg/kg of the respective 8kDa hPG amine (Figure 3). For this purpose 786-O-Luc tumor cells subcutaneously inoculated into NMRI nu/nu mice and with an average size of ~50 mm^2 were intratumorally injected with 8kDa hPG amine polyplexes on three consecutive days (day 0 – day 2). The transfection efficacy was determined by changes of the luciferase activity (% of day 0) 24 h after each injection, respectively.

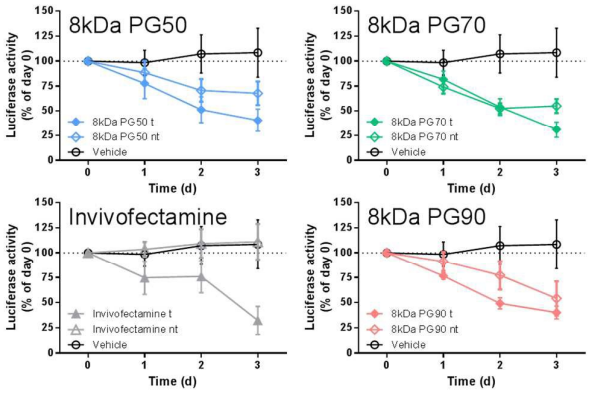

Figure 3. *In vivo* knockdown study with 8kDa hPG amines: silencing of the luciferase gene was investigated after intratumoral injection of 8 mg/kg 8kDa PG50, 8kDa PG70 or 8kDa PG90 complexed with luciferase-specific siRNA (t) or non-targeting siRNA (ON-TARGETplus Non-targeting siRNA, Dharmacon) (nt) at N/P ratios of 10, 8, and 3 respectively in NMRI nu/nu mice bearing 786-O Luc tumors. Invivofectamine 2.0 Reagent complexed with anti-Luc siRNA and non-targeting siRNA was used as technical control. As negative control (vehicle) HyClone™ HyPure water was injected. The results are shown as mean ± SD of triplicates. Bioluminescence of tumors was determined after i.p. administration of 50 mg/kg D-Luciferin (PerkinElmer).

The consecutive administration of the 8kDa hPG amines complexed with anti-Luc siRNA and non-targeting siRNA induced a reduced luciferase activity starting at d1 vs. d0. Here, the strongest effect has been detected at day 3 revealing approximately 60%, 69% and 60% inhibition by 8kDa PG50, 8kDa PG70 and 8kDa PG90 complexed with anti-Luc siRNA, respectively. In contrast, the technical control Invivofectamine complexed with anti-Luc siRNA inhibited the expression of the luciferase up to 68% at day 3, which was not seen by the non-targeting siRNA. HyClone™ HyPure water did not affect the tumor bioluminescence. Surprisingly, the impact of the amine multiplicity reflected by the different *in vitro* transfection efficacies of the tested 8kDa hPG amines could not be confirmed *in vivo*. However, treatment with 8kDa hPG amines revealed an inhibition of luciferase activity independent of the complexed siRNA indicating unspecific side effects *in vivo* by consecutive injection. Conclusively, we could demonstrate that increasing the amine loading while keeping the core size leads to an improved effective charge density. This resulted in an optimized nanocarrier 8kDa PG90 with the best multiplicity/charge density balance enabling high knockdown effects *in vitro*. Unfortunately, 8kDa PG90 showed limited tolerability after systemic administration by inducing the secretion of pro-inflammatory cytokines and by leading to an unspecific reduction of the luciferase activity during *in vivo* knockdown studies.

43kDa hPG amine with improved knockdown efficacy *in vivo*

In order to proof our hypothesis that increasing the size of a macromolecular architecture improves specificity while enhancing tolerability without reducing knockdown efficacy, the larger core hPG amine 43kDa PG50 was characterized compared to 8kDa PG90 *in vitro* and *in vivo*. Both scaffolds have a comparable amount of amine groups per surface area but different charge densities (Supporting Information, Table S 1). The proposed difference in the charge density of 8kDa PG90 and 43kDa PG50 was equally confirmed. 43kDa PG50 revealed a zeta-potential of approximately 16 mV at N/P 1, while the zeta-potential of 8kDa PG90 was 5 mV at N/P1 (Supporting Information, Figure S 3). Further, determination of the hydrodynamic size and gel electrophoresis measurements confirmed a stable polyplex formation at N/P 3 for both hPG amines, 43kDa PG50 and 8kDa PG90, enabling a comparative *in vitro* and *in vivo* investigation (Supporting Information, Figure S 1 & S 3). The evaluation of transfection efficacy and tolerability *in vitro* revealed no reduction of cell viability and a decrease of the luciferase activity of 17% by 43kDa PG50/anti-luciferase siRNA complexes and of 30% by 8kDa PG90 complexed with anti-luciferase siRNA (Supporting Information, Figure S6).

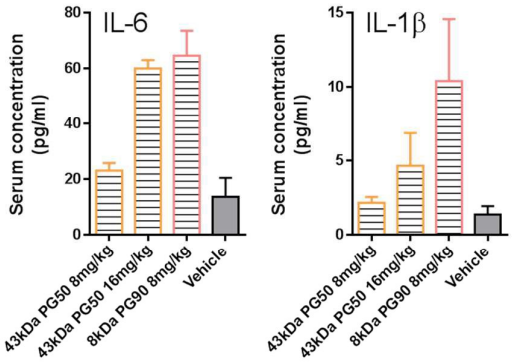

Figure 4. Determination of pro-inflammatory cytokine levels after systemic administration of 8kDa PG90 vs. 43kDa PG50: three BALB/c mice per group were treated intravenously with 8 mg/kg or 16 mg/kg 43kDa PG50 or 8 mg/kg 8kDa PG90 complexed with non-targeting siRNA at a N/P ratio of 3. HyClone™ HyPure water was used as negative control (vehicle). Retrobulbar blood was taken 1h after injection and serum was examined via Meso Scale Discovery Multi-Spot Assay System, Mouse ProInflammatory 7-Plex Assay Ultra-Sensitive Kit. Results are shown as mean±SD of triplicates.

Hence, the *in vitro* transfection efficacy did not improve with the effective charge density as opposed to our expectations. That can be explained by limited molarity of polyplexes in cell-based assays. To further investigate the impact of the effective charge density on the tolerability of 43kDa PG50 *in vivo,* pro-inflammatory cytokine levels after systemic injection were determined (Figure 4 and Supporting Information, Figure S 7). The intravenous administration of 8 mg/kg 43kDa PG50 revealed a comparable acute immune response to the vehicle control (Figure 4) and remarkably, even the double dose (16 mg/kg) of 43kDa PG50 caused less secretion of i.e. IL-1β and IL-6 compared to 8 mg/kg 8kDa PG90. In conclusion, the increased core size and subsequently improved effective charge density of 43kDa PG50 lead to a better tolerability *in vivo,* enlarging its therapeutic benefit. These findings prove our hypothesis that an enhanced tolerability is a result of the enhanced effective charge density as a result of the increased hydroxyl to amine group ratio.The increased tolerability of 43kDa PG50 enabled the investigation of the gene silencing

potential in tumor bearing mice at 8 mg/kg and 16 mg/kg in comparison to the maximal tolerable dose of 8 mg/kg for 8kDa PG90. HyClone™ HyPure water and Invivofectamine were used as negative and technical control, respectively. Neither the animal weight nor the tumor growth has been affected by the intratumoral injection of the different 8kDa PG90 and 43kDa PG50 complexes as well as the respective control on three consecutive days (Supporting Information, Figure S8). In addition, histological analysis revealed no changes of the tumor tissue structure irrespective of administered nanotransporter (Supporting Information, Figure S 9).

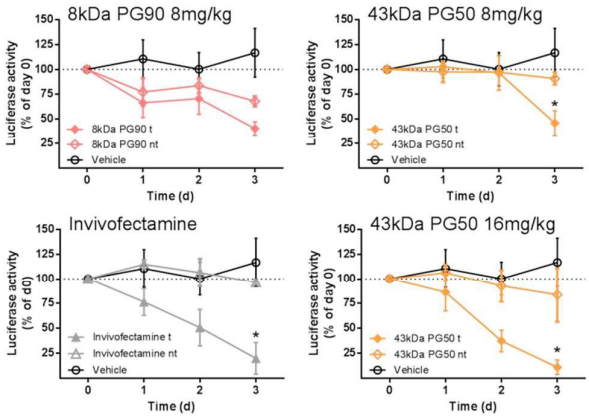

Figure 5. *In vivo* knockdown study with 43kDa PG50 vs. 8kDa PG90: *In vivo* silencing of the luciferase gene was investigated after intratumoral injection of 8 mg/kg 8kDa PG90 and 8 mg/kg or 16 mg/kg 43kDa PG50, respectively, complexed with luciferase specific siRNA (t) or non-targeting siRNA (nt) at N/P ratio 3 in NMRI nu/nu mice bearing 786-O Luc tumors. Invivofectamine 2.0 Reagent (IF) complexed with anti-Luc siRNA was used as technical control and HyClone™ HyPure water as negative control (vehicle). The results are shown in mean±SD, n=4. Statistical analysis was performed to compare the luciferase activity of tumors treated with anti-Luc siRNA and those with non-targeting siRNA on day 3 by using the unpaired one-sided t-test with logarithmized data (* $p<0.05$)

Analysis using TUNEL and Ki-67 additionally showed no effect on the number of apoptotic cells and proliferative cells following siRNA/nanoparticle administration, respectively, indicating that hPG amines do not induce considerable cytotoxic effects. In contrast to the treatment with 8kDa PG90, the light emission of the tumors treated with 8 mg/kg 43kDa PG50 polyplexes was target-specific and significantly reduced to 54% on day 3 vs. day 0. The knockdown effect was further enhanced by the administration of 16 mg/kg 43kDa PG50/anti-Luc complexes (Figure 5). Thereby, the luciferase activity of tumors treated with 16 mg/kg anti-Luciferase siRNA/43kDa PG50 polyplexes was significantly reduced by 89% compared to the non-targeting control (16%) at day 3 (Figure 5 and 6). Interestingly, 43kDa PG50 (16 mg/kg) revealed a stronger knockdown effect than the technical control Invivofectamine, which induced an inhibition of 80% in our study. Hence, 43kDa PG50 is at least equivalent or superior to the commercial product Invivofectamine, which represents a lipid-based gene delivery vector. In conclusion, this knockdown study proves the high potential of 43kDa PG50 as a well-tolerated and highly efficient nanoparticle for siRNA delivery *in vivo*.

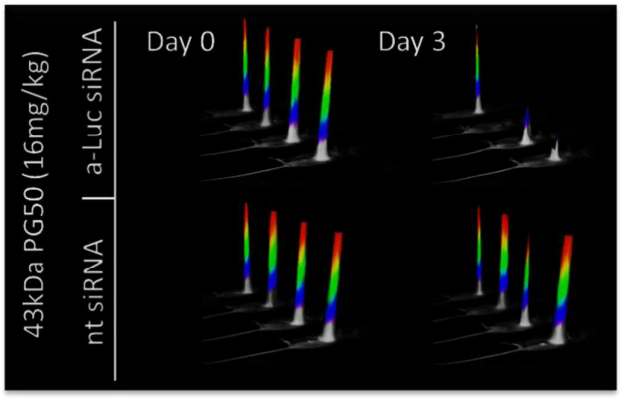

Figure 6. 3D bioluminescence image of mice treated with 16mg/kg 43kDa PG50: light emission of tumors before (day 0) and after (day 3) treatment with 16 mg/kg 43kDa PG50 complexed with non-targeting (nt) siRNA and luciferase specific (a-Luc) siRNA, respectively on three consecutive days.

Determining the ratio between the mean value of the luciferase activity of tumors treated with non-targeting siRNA and those treated with anti-Luc siRNA on day 3 (effect size) underlined the high and target-specific potency of 43kDa PG50 vs. the 8kDa PG amines (Figure 7). The 8kDa PG50, PG70 and PG90 revealed a small effect size of 3.2, 2.4 and 1.8, respectively, whereas 16 mg/kg of 43kDa PG50 had an effect size of 44. Remarkably, Invivofectamine as technical control showed a lower effect size of 33, which emphasizes the strong and highly significant knockdown effect of 43kDa PG50 (16 mg/kg). Finally, we studied the impact of 43kDa PG50 on the knockdown of endogenous polo-like kinase-1 (PLK-1) in 786-O-Luc tumors. PLK-1 is crucial for cell division by promoting mitotic entry and controlling mitotic progression in mammalian cells.[35] Depletion of the PLK-1 using RNA interference has been reported to be capable of inducing anti-tumor effects.[36] 43kDa PG50 (16 mg/kg) complexed with PLK-1 specific and non-targeting siRNA, respectively, was intratumorally administered on three consecutive days (day 0 – day 2). HyClone™ HyPure water served as negative control. The progression of tumor growth was noninvasively monitored by detecting bioluminescence on day 3. The light emission was significantly reduced by 80% on day 3 vs. day 0 due to the administration of the 43kDa PG50/anti-PLK-1 siRNA, whereas polyplexes with non-targeting siRNA induced no decrease of bioluminescence compared to day 0 (Supporting Information, Figure S10). These findings confirmed the target specific and highly efficacious silencing effect of 43kDa PG50.

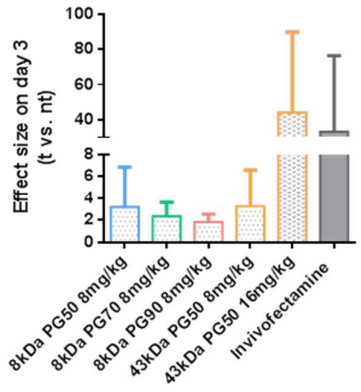

Figure 7. Determination of the effect size of all evaluated nanoparticles: the effect size reflects the ratio between the mean values of the luciferase activity of tumors treated with anti-Luc siRNA (t) vs. non-targeting siRNA (nt) on day 3 complexed with 8mg/kg 8kDa PG50, 8mg/kg 8kDa PG70, 8mg/kg 8kDa PG90, 8mg/kg 43 kDa PG50, 16mg/kg 43kDa PG50 and the technical control Invivofectamine.

Materials and methods

General synthesis of hPG amines

All starting materials were commercially available. The absolute solvents were used without further purification. Glycidol was dried over CaH_2, distilled under reduced pressure, and stored under argon atmosphere at 4 °C. Air and moisture sensitive reactions were conducted using glassware dried at 300 °C and flushed with argon, respectively, three times just before the reaction. Addition of chemicals was carried out under inert gas. The synthesis of the high molecular weight polyglycerol was established similar to the lately published findings of Brooks et al.[37] The low molecular weight polyglycerol (8 kDa) was provided following the published synthesis.[38] The degree of branching (DB) of all polymers was calculated out of the inverse gated 13C-NMR measurements using an equation from literature.[29]

High molecular weight (HMW) PG synthesis: The reaction was performed in a 100 mL three-necked flask with a KPG-stirrer, dried under heating, and flushed with argon, respectively. The amount of 1,1,1 - Tris(hydroxylmethyl)propane (TMP) (1.23 mmol, 165 mg) was added and dried for another 15 min at 95 °C. To the reaction mixture potassium methanol (0.36 mmol, 105 µL) was added under argon and kept for 45 min at 95 °C to get rid of the methanol. Finally Tetrahydropyran (THP) (6 mL) was added and the suspension was stirred for 30 min at 85°C, to get all compounds into solution. Glycidol (180 mmol, 12 mL) was added over 8.6 h (1.4 mL/h). The reaction was stirred overnight at 85°C, quenched with 30 mL methanol, and stirred for another 30-45 min until the reaction mixture was completely dissolved. The solvent was evaporated and the mixture was dissolved in 100 mL methanol. The ion exchanger (Amberlite IR120) was activated with a 5M HCl solution and washed two times with 200 mL methanol before use. A column was prepared with the activated ion exchanger and the reaction mixture was flashed at least five times through the ion exchanger under gravity with increasing solvent (100 mL-1.0 L). All solvent was evaporated, the product was dissolved in 20 mL methanol and dialyzed for 3 d (Solvent: methanol). Finally the product was dried under HV for 1 d to get a colorless highly viscous liquid. Yield: 67%, molecular weight distribution (GPC): M_n (43 Da), M_w (99 Da), M_p (75 Da), PDI: 1.9, DB: 60%. ^{1}H-NMR (CD_3OD, 700 MHz): δ = 4.1-3.5 ppam (m, PG-Backbone), ^{13}C-NMR (CD_3OD, 176 MHz): δ = 79.43 (hPG backbone, linear 1–3 units), 78.00 (hPG backbone, dendritic units), 72.16 (hPG backbone, linear 1–4 units), 70.71-70.43 (hPG backbone, linear/dendritic units), 69.19-68.90 (hPG backbone, linear 1–3/1–4 units), 62.61 (hPG backbone, terminal units) and 60.76 (hPG backbone, linear 1–3 units).

The surface modification of the hydroxyl groups was performed according to the published procedure.[30] In short: hPG (1 g, 13.5 mmol OH groups) was dissolved in abs. pyridine (15 mL). The solution was cooled down to 0 °C using an ice/sodium chloride bath,and a solution of mesylchloride (0.5 mL, 0.77 g, 6.75 mmol) was added. After reprocessing the gained O-Mesylpolyglycerol was dissolved in p.a. DMF and to the mixture NaN_3 (4.39 g, 5 eq) was added. The reaction mixture was stirred overnight at 60 °C and finally dialyzed in methanol. In the last step, the polyglycerolazide was reduced to hPG amine using PPh_3 (1.77 g, 6.75 mmol, 1 eq) in p.a. THF/H_2O (1:1).

Step 1: Conversion: quant., yield: 85%; ^{1}H-NMR (400 MHz, $(CD_3)_2CO$), δ: 5.16 − 4.74 (functionalized secondary OH-groups, nPG), 4.63−4.20 (functionalized primary OH-groups, nPG), 3.17 (Me); IR (KBr): ν = 3030(w), 2941(m), 1709(w), 1457(w), 1362(w), 1184(m), 971(ν_s), 813(m), 753(m) cm^{-1}.

Step 2: Conversion: quant., yield: 86%; ^{1}H-NMR (400 MHz, $CDCl_3$) δ: 4.23–2.87 (PG-backbone); IR (KBr): ν = 2873(w), 2102 (s, (N_3)), 1457(w), 1273(m), 1122(m), 668(m) cm^{-1}.

*Step 3:*Conversion: quant.; yield: 85%; ^{1}HNMR (400 MHz, CD_3OD) δ: 4.2–3.5 (PG-backbone), 3.4–3.2 (functionalized PG-groups); IR (KBr): ν = 3354(w), 2874(m), 1576(s), 1473(m), 1338(m), 1104(m), 820(m), 668(m) cm^{-1}.

Analytical Measurements

Dialysis was done in benzoylated cellulose dialysis tubes from Sigma-Aldrich (No. D-7884, width: 32nm, molecular weight cut-off ((MWCO) 1000 g mol^{-1}). NMR spectra were obtained using the following spectrometers: Bruker ECX 400 (400 MHz proton-resonance) and Bruker AVANCE 700 (700 MHz proton-resonance, solvent standards, sample amount: ^{1}H-NMR: 5-15 mg, ^{13}C-NMR: 40-80 mg). IR spectra were performed by using a FT/IR-4100 LE 170VA (Jasco Cooperation, Groß-Umstadt, Germany). All samples were measured as highly viscous liquids using one drop of the concentrated pure compound directly onto the diamond and were carried out under air conditions at 25 °C. Before every measurement the background was premeasured and automatically subtracted. All the spectra were analyzed by the given software “Spectra Manager”.

Gel permeations chromatography (GPC)

The molecular weight distribution was determined by means of GPC coupled to a multiangle laser light scattering (MALLS) - and a refractive index (RI) detector. The complete distribution (M_n, M_p, M_w, M_w/M_n) was obtained using highly diluted conditions (10 mg mL^{-1}, injected volume 20 µL) from the GPC consisting of an Agilent 1100 solvent delivery system with isocratic pump, a manual injector, and an Agilent differential refractor meter. Three 30 cm columns (Polymer Laboratories PFgel Mixed C, 5 µm particle size) were used to separate aqueous polymer samples using water with 0.05% NaN_3 as mobile phase at a flow rate of 1 mL min^{-1}. The columns were operated at 25 °C with the detectors at 50 °C. The calibration was performed by using certified standard Pullulan (linear) from PSS. WinGPC Unity from PSS was used for data acquirement and interpretation. All measurements were only performed for the hyperbranched polyglycerol cores.

Dynamic light scattering and zeta-potential

Dynamic light scattering (DLS) measurements were obtained using Malvern Zetasizer Nano ZS (Malvern Instruments GmbH, Herrenberg, Germany). All samples were measured at a constant scattering angle of 173°, 25 °C, and freshly prepared just before measurement in either HyClone™ HyPure water (pH 6.5-7.5) or PBS-buffer (10 mM, pH 7.4, Fischer Bio Reagents) for the hydrodynamic size and zeta-potential measurements. All the measurements were repeated at least three times. The polyplexes were prepared at the requested N/P ratio by adding to a siRNA solution (150 nmol mL^{-1}, On-Target plus® non-targeting siRNA) the correlated amount of hPG amine. The polyplex were incubated for 30 min at 25 °C and then diluted with either HyClone™ HyPure water or PBS-buffer to 0.7 mL for the zeta-potential measurements. Slightly turbid solutions were formed at N/P ratio 6 to 10 for 43kDa PG50.

Gel electrophoresis studies

Gel electrophoresis studies were performed using the instrument gel doc station (Gel XL Ultra electrophoreses system, Labnet international Inc., Edison, USA). The gel was prepared using the following procedure; 1 g of agarose powder was dissolved in 100 mL HEPES buffer (2 mmol HEPES, 10 pmol EDTA, 9.4 mmol sodium chloride, pH-value of 7.4) and heated in a microwave three times for 1 min at 100 °C. After 10 min of cooling 2 µL of 1% ethidium bromide solution in HEPES buffer was added to the gel and stirred for 1 min to get a homogenous mixture. The gel was filled into the gel XL ultra-shape, a comb was fixed to finally get the basins for the polyplex solution, and after another 30 min of cooling the gel became firm. Finally the gel was covered slightly with HEPES buffer. The polyplexes were prepared as already mentioned in the DLS section and a total volume of polyplex (20 µL) was filled into the basins. The measurements were programmed for 30 min by 50 V. All pictures of the fractions in the gel were obtained using the fixed gel onto the UV sample tray at a wavelength of 254 nm. The pictures were taken with a digital camera (EOS 350D) and processed with *"Corel Photo Paint X5"*.

Cell culture

The human renal carcinoma cell line 786-O-Luc, constitutively expressing the firefly luciferase, was used for transfection and cell viability studies. 786-O-Luc cells were generated by stable transfection in-house (Bayer Healthcare, GDD, Global Therapeutic Research) and cultured in growth medium composed of RPMI 1640 (Biochrom), supplemented with 10% FCS, 1% 200 mM glutamine, 1% 100 mM pyruvat, 1% 1 M HEPES, 4.5 g L^{-1} glucose and 50 µg mL^{-1}hygromycine B at 37°C, 5% CO_2.

Transfection and cell viability assay

The cell viability was investigated in 786-O-Luc tumor cells following hPG amine treatment, respectively. Cells were cultured in 96-well plates at a density of 1 x 10^4 cells per well. After 24 hours the growth medium was discarded and replaced by 100 µL Opti-MEM (Gibco). The hPG amines were dissolved in water and complexed with luciferase specific (GCAAGAUCGCCGUGUAAUAUU, Dharmacon) or non-targeting siRNA (ON-TARGETplus Non-targeting siRNA, Dharmacon) by incubating 5 pmol siRNA with corresponding amounts of nanocarriers depending on N/P ratios. Lipofectamine RNAiMAX transfection reagent (Invitrogen) was used as a technical control following the manufacturer's protocol. Untreated cells were used as the negative control. In a total volume of 50 µL the polyplexes were added to the cells and incubated for 24 h at 37°C, which was then replaced by RPMI growth medium and incubated for another 24 h.
The transfection efficacy of the nanocarriers was examined via quantitation of firefly luciferase reporter gene activity from treated 786-O-Luc cells. To determine the number of viable cells simultaneously within this study, the ONE-Glo™ + Tox Luciferase Reporter and Cell Viability Assay (Promega) was used pursuant to the manufacturer's protocol. Luminescent and fluorescent signals were detected via Tecan Infinite 200Pro.

Determination of pro-inflammatory cytokines

To determine the acute effect of hPG amines on the cytokine secretion *in vivo*, three BALB/c mice (Charles River) per group were treated intravenously (i.v.) at doses of 8 mg/kg and 16 mg/kg, respectively, complexed with non-targeting siRNA (ON-TARGETplus Non-targeting siRNA, Dharmacon) at N/P 3, 8 and 10. Invivofectamine 2.0 Reagent (Invitrogen) was complexed with non-targeting siRNA according to the manufacturer's manual and used as technical control. HyClone™ HyPure water was administered as negative control. Retrobulbar blood was taken 1 h after administration and the serum was harvested. Cytokine levels in the serum were determined using the Meso Scale Discovery Multi-Spot Assay System, Mouse ProInflammatory 7-Plex Assay Ultra-Sensitive Kit corresponding to manufacturer's protocol.

Knockdown of luciferase and PLK-1 gene *in vivo*

The *in vivo* knockdown efficacy of the hPG amines was evaluated by using the 786-O-Luc tumor xenograft model.

Therefore, female NMRI nu/nu mice (Janvier) aged 6-8 weeks were inoculated subcutaneously (s.c.) with $2x10^6$ 786-O-Luc cells in 100µl Matrigel (BD), and the tumor growth was monitored by caliper measurement.
NMRI nu/nu mice bearing ~50 mm^2 786-O-Luc tumors were injected intratumorally with 8 mg/kg or 16 mg/kg 8kDa PG50, 8kDa PG70, 8kDa PG90 and 43kDa PG50, respectively, complexed with luciferase specific (GCAAGAUCGCCGUGUAAUAUU, Dharmacon), PLK-1 specific (siGENOME Human PLK1 siRNA – SMARTpool, Dharmacon) or non-targeting siRNA (ON-TARGETplus Non-targeting siRNA, Dharmacon). Invivofectamine 2.0 Reagent (Invitrogen) was complexed with luciferase specific or non-targeting siRNA according to the manufacturer's manual and used as the technical control. HyClone™ HyPure water was administered as negative control. Every group consisted of 3 or 4 animals. Polyplexes were injected daily for three consecutive days. Animals were monitored every other day after treatment for tumor area. The luciferase activity of the tumors was determined by using the bioluminescence imaging system (Nightowl, Berthold Technologies) after intraperitoneal injection of 50 mg/kg Luciferin (D-Luciferin Firefly, potassium salt, PerkinElmer). Images were analyzed via Indigo software (Berthold Technologies).

Immunohistochemistry

All specimens were kept in 10% buffered formalin for 48 hours, followed by embedding in paraffin. Slides with a thickness of 3 µm were prepared and deparaffinized sections were soaked in alcohol. After steam cooker treatment in antigen unmasking solution at 125°C for 30 seconds they were incubated in 1,5% hydrogen peroxide for 10 minutes. After staining with the appropriate antibody, epitopes were detected using the Dako REAL Detection System (Dako). The proliferation of 786-O tumor cells was determined by staining tumor sections with an anti-Ki-67 antibody (Abcam) diluted 1:150. The extent of apoptosis in the tumor sections was measured by TUNEL using the ApopTag Peroxidase *in Situ* Apoptosis Detection Kit (Millipore), following the manufacturers protocol. The slides were counterstained with Mayer's hematoxylin. Slides were scanned using the Zeiss Mirax Midi Slide Scanner and analyzed with the Mirax Viewer Software.

Conclusions

In this work we have shown for the first time that the balance between core size, multiplicity and effective charge density plays an important role for the development of potent siRNA delivery vectors. The designed hyperbranched polyglycerol amines were modified in their effective functionality by balancing charge density and multiplicity demonstrated *in vivo*. Investigations of high molecular weight hPG amine 43kDa PG50 revealed weaker pro-inflammatory immune responses after systematic application compared to the small core hPG amine 8kDa PG90 with low effective charge density. This is in contrast to polyethylenimines, where only small oligomers are tolerated *in vivo*. The enhanced tolerability allowed not only a higher dosing for *in vivo* knockdown studies but also resulted in a strong and significant silencing of the luciferase gene in tumor bearing mice. Therefore, the newly designed hPG amine 43 kDa PG50 represents a promising candidate for siRNA delivery and for addressing of so far "undruggable" targets.

Acknowledgements

The "Bundesministerium für Bildung und Forschung" (BMBF) and the "Sonderforschungsbereich SFB 765" are kindly acknowledged for financial support. We thank Christine Willrich and Dr. Ana C. Rodrigo for support, and Dr. Florian Paulus for providing the low molecular polyglycerol core (8kDa).

Notes and references

‡ All *in vivo* experiments were performed according to the German animal protection law.

1 J. Zhou, H. Li, S. Li, J. Zaia and J. J. Rossi, *Mol. Ther.*, 2008, **16**, 1481–1489.

2 A. L. Hopkins and C. R. Groom, *Nat. Rev. Drug Discov.*, 2002, **1**, 727–30.

3 M. E. Davis, *Mol. Pharm.*, 2009, **6**, 659–68.

4 K. A. Whitehead, R. Langer and D. G. Anderson, *Nat. Rev. Drug Discov.*, 2009, **8**, 129–38.

5 C. Huang, M. Li, C. Chen and Q. Yao, *Expert Opin. Ther. Targets*, 2008, **12**, 637–45.

6 J. Zhou, J. Wu, N. Hafdi, J.-P. Behr, P. Erbacher and L. Peng, *Chem. Commun. (Camb).*, 2006, 2362–4.

7 E. Wagner, *Acc. Chem. Res.*, 2012, **45**, 1005–1013.

8 X. Guo and L. Huang, *Acc. Chem. Res.*, 2012, **45**, 971–979.

9 A. Wittrup and J. Lieberman, *Nat. Rev. Genet.*, 2015, **16**, 543–552.

10 J. Khandare, M. Calderón, N. M. Dagia and R. Haag, *Chem. Soc. Rev.*, 2012, **41**, 2824.

11 D. Wang, T. Zhao, X. Zhu, D. Yan and W. Wang, *Chem. Soc. Rev.*, 2015.

12 M. Morille, C. Passirani, A. Vonarbourg, A. Clavreul and J. P. Benoit, *Biomaterials*, 2008, **29**, 3477–3496.

13 M. Mintzer and E. E. Simanek, *Chem. Rev.*, 2009, **109**, 259–302.

14 P. L. Felgner, T. R. Gadek, M. Holm, R. Roman, H. W. Chan, M. Wenz, J. P. Northrop, G. M. Ringold and M. Danielsen, *Proc. Natl. Acad. Sci. U. S. A.*, 1987, **84**, 7413–7417.

15 D. Zhi, S. Zhang, S. Cui, Y. Zhao, Y. Wang and D. Zhao, *Bioconjug. Chem.*, 2013, **24**, 487–519.

16 J. Behr, *Chim. Int. J. Chem.*, 1997, **2**, 34–36.

17 M. Breunig, U. Lungwitz, R. Liebl and A. Goepferich, *Proc. Natl. Acad. Sci. U. S. A.*, 2007, **104**, 14454–14459.

18 K. Kunath, *J. Control. Release*, 2003, **89**, 113–125.

19 S. Werth, B. Urban-Klein, L. Dai, S. Höbel, M. Grzelinski, U. Bakowsky, F. Czubayko and A. Aigner, *J. Control. Release*, 2006, **112**, 257–70.

20 T. Bieber, W. Meissner, S. Kostin, A. Niemann and H. P. Elsasser, *J. Control. Release*, 2002, **82**, 441–454.

21 D. Fischer, Y. Li, B. Ahlemeyer, J. Krieglstein and T. Kissel, *Biomaterials*, 2003, **24**, 1121–1131.

22 X. Liu, P. Rocchi and L. Peng, *New J. Chem.*, 2012, **36**, 256.

23 T. Yu, X. Liu, A.-L. Bolcato-Bellemin, Y. Wang, C. Liu, P. Erbacher, F. Qu, P. Rocchi, J.-P. Behr and L. Peng, *Angew. Chem. Int. Ed. Engl.*, 2012, **51**, 8478–84.

24 R. V Benjaminsen, M. a Mattebjerg, J. R. Henriksen, S. M. Moghimi and T. L. Andresen, *Mol. Ther.*, 2012, **21**, 149–157.

25 O. Boussif, F. Lezoualc'h, M. Zanta, M. D. Mergny, D. Scherman, B. Demeneix and J. P. Behr, *Proc. Natl. Acad. Sci. U. S. A.*, 1995, **92**, 7297–7301.

26 W. Fischer, M. Calderón, A. Schulz, I. Andreou, M. Weber and R. Haag, *Bioconjug. Chem.*, 2010, **21**, 1744–1752.

27 P. Ofek, W. Fischer, M. Calderón, R. Haag and R. Satchi-Fainaro, *FASEB J.*, 2010, **24**, 3122–3134.

28 W. Fischer, M. Calderón and R. Haag, *Top. Curr. Chem.*, 2010, **296**, 95–129.

29 A. Sunder, H. Frey and R. Mülhaupt, *Macromol. Symp.*, 2000, **153**, 187–196.

30 S. Roller, H. Zhou and R. Haag, *Mol. Divers.*, 2005, **9**, 305–316.

31 D. Peer, J. M. Karp, S. Hong, O. C. Farokhzad, R. Margalit and R. Langer, *Nat. Nanotechnol.*, 2007, **2**, 751–760.

32 E.-J. Park and K. Park, *Toxicol. Lett.*, 2009, **184**, 18–25.

33 Y. Zhang, N. Chirmule, G. P. Gao, R. Qian, M. Croyle, B. Joshi, J. Tazelaar and J. M. Wilson, *Mol. Ther.*, 2001, **3**, 697–707.

34 L. Zhang, F. X. Gu, J. M. Chan, A. Z. Wang, R. S. Langer and O. C. Farokhzad, *Clin. Pharmacol. Ther.*, 2008, **83**, 761–9.

35 E. Kawata, E. Ashihara, S. Kimura, K. Takenaka, K. Sato, R. Tanaka, A. Yokota, Y. Kamitsuji, M. Takeuchi, J. Kuroda, F. Tanaka, T. Yoshikawa and T. Maekawa, *Mol. Cancer Ther.*, 2008, **7**, 2904–12.

36 X. Liu and R. L. Erikson, *Proc. Natl. Acad. Sci. U. S. A.*, 2003, **100**, 5789–94.

37 M. I. Ul-Haq, R. Shenoi, D. E. Brooks and J. N. Kizhakkedathu, *J. Polym. Sci. Part A Polym. Chem.*, 2013, **51**, 2614–2621.

38 F. Paulus, M. E. R. Weiss, D. Steinhilber, A. N. Nikitin, C. Schütte and R. Haag, *Macromolecules*, 2013, **46**, 8458–8466.